

Adaptive Slimming for Scalable and Efficient Speech Enhancement

Riccardo Miccini^{b#}, Minje Kim^b, Clément Laroche^b, Luca Pezzarossa[#], Paris Smaragdis^b

^bGN Audio, Denmark; ^bUniversity of Illinois at Urbana-Champaign, USA; [#]Technical University of Denmark, Denmark

Abstract—Speech enhancement (SE) enables robust speech recognition, real-time communication, hearing aids, and other applications where speech quality is crucial. However, deploying such systems on resource-constrained devices involves choosing a static trade-off between performance and computational efficiency. In this paper, we introduce dynamic slimming to DEMUCS, a popular SE architecture, making it scalable and input-adaptive. Slimming lets the model operate at different utilization factors (UF), each corresponding to a different performance/efficiency trade-off, effectively mimicking multiple model sizes without the extra storage costs. In addition, a router subnet, trained end-to-end with the backbone, determines the optimal UF for the current input. Thus, the system saves resources by adaptively selecting smaller UF when additional complexity is unnecessary. We show that our solution is Pareto-optimal against individual UF, confirming the benefits of dynamic routing. When training the proposed dynamically-slimmable model to use 10 % of its capacity on average, we obtain the same or better speech quality as the equivalent static 25 % utilization while reducing MACs by 29 %.¹

Index Terms—speech enhancement, dynamic neural networks, edge AI

1. INTRODUCTION

Speech enhancement (SE) systems are a crucial part of telecommunication, teleconferencing, and assistive technology, improving remote collaboration, user experience, and quality of life. In recent years, SE solutions based on deep learning made significant progress, thanks to their ability to learn from vast amounts of data [1]–[6]. However, deploying these systems on resource-constrained embedded devices such as headsets, speakerphones, or hearing aids requires a careful trade-off between denoising performance and computational needs. This can be challenging to achieve, given the broad range of acoustic conditions and noise levels experienced in the real world. Because devices must handle rare but challenging acoustic scenarios without failing, they require sufficiently large models trained from a large dataset for worst-case conditions. Consequently, in typical scenarios that involve relatively clean inputs, SE models are over-provisioned, wasting computational resources and energy.

Dynamic neural networks (DynNN) offer a solution to this problem, providing specialized architectures and training strategies to develop artificial neural networks that can manipulate certain aspects of their computational graph at inference time, often based on the input [7]. DynNNs with scalable depth, width, or adaptive/conditional connections have been successfully applied to computer vision [8]–[12] and, as of recently, are being investigated on audio-processing tasks [13]–[16]. In this paper, we introduce *dynamic slimming* to DEMUCS [17], a popular SE architecture, to make it scalable and input-adaptive. Slimming is a form of width-wise dynamism that lets the model operate at different *utilization factors* (UF), corresponding to discrete subsets of weights, each providing a different performance/efficiency trade-off. Intuitively, higher UF corresponds to larger networks, resulting in better denoising performance, but at higher computational costs. This is conceptually equivalent to deploying multiple models of different sizes without incurring the

This work has received funding from the European Union’s Horizon research and innovation program under grant agreement No 101070374.

¹Samples at <https://miccio-dk.github.io/adaptive-slimming-speech-ench/>

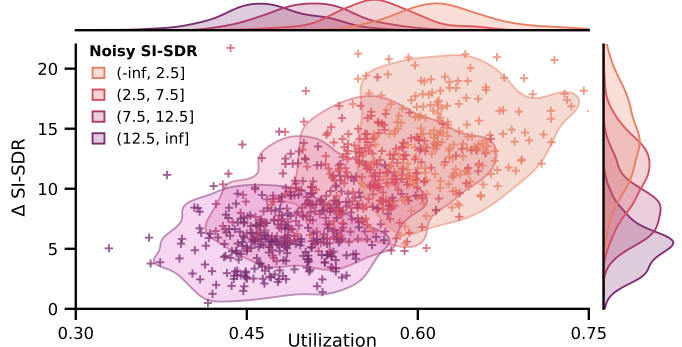


Fig. 1: Relationship between average utilization and SI-SDR improvement for model trained with $v_{trgt} = 0.5$, showing how our proposed solution processes noisier input data (lighter points) using more resources, causing a larger improvement.

cost of storing all their weights, such as a sparse mixture of local experts for SE [18], thanks to its structured architecture.

We hypothesize that the UF concept is associated with the difficulty of the SE task. Input noise conditions can range from easy (e.g., high SNR or static noise) to more challenging (e.g., low SNR, non-stationary, or speech-like noise). Thus, using a large model across a range of SE tasks can induce redundancy in its architecture, wasting resources when the input is trivial. In our work, a routing module estimates the optimal UF for each utterance based on the input characteristics and a desired average utilization target, ensuring an advantageous trade-off between computational efficiency and speech quality by selecting smaller UF when larger ones would offer limited additional benefits (as demonstrated in Fig. 1). The resulting system is an adaptively-slimmable neural network that can match the denoising performance of a given static baseline while using fewer computational resources on average. We also observe that dynamic routing is Pareto-optimal when compared with statically selecting a specific UF because, by adapting to the input, the proposed system selects the most advantageous trade-off points, reducing the average computational costs. We contribute the following: 1) Performance and efficiency improvements on the DEMUCS baseline and architectural adaptations to support multiple performance/efficiency trade-offs through slimming; 2) Design of a lightweight routing sub-network for input-dependent scalability, along with training strategy; 3) Model evaluation with respect to its training hyperparameters.

2. RELATED WORK

Efficient speech enhancement Over the years, several deep learning models for SE have demonstrated real-time capabilities. These efficient SE models may integrate architectural elements such as multi-path processing [3], [5], [19] or encoder-decoder topology with skip connections [4], [6], [20], [21] based on U-Net [22]. Some of these architectures, often based on recurrent networks [1], have been specifically optimized for embedded devices [2], [23].

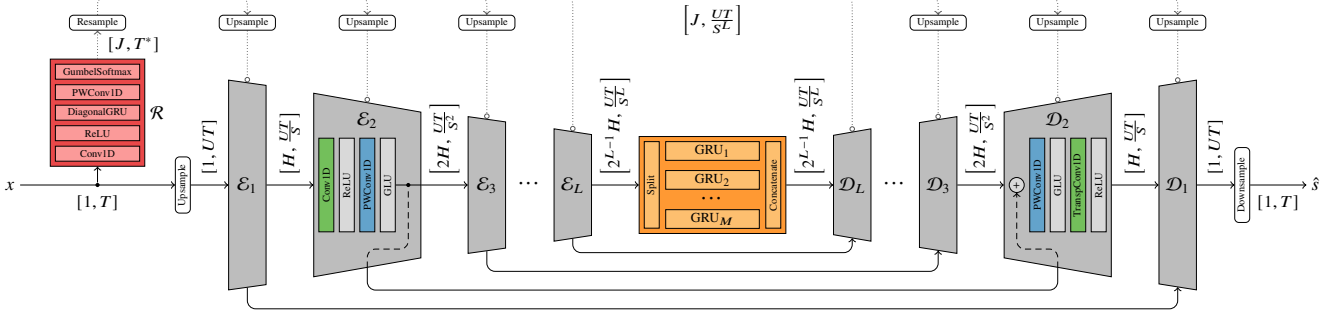


Fig. 2: Overall solution showing DEMUCS backbone with encoder \mathcal{E}_i and decoder \mathcal{D}_i blocks (gray), the grouped GRU bottleneck (orange), and routing subnet \mathcal{R} (red). Connections between blocks are annotated with signal dimensionality. Dotted connections represent UF arguments.

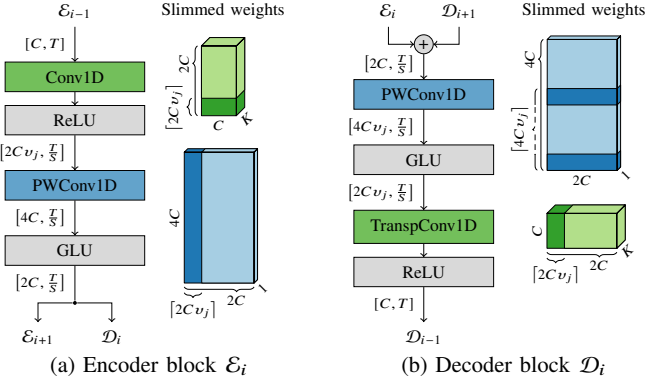


Fig. 3: Slimmable blocks with weight tensors; width, height, and depth correspond to input channels, output channels, and kernel size, respectively; $C = 2^{i-2}H$ for $i \geq 2$ is the current hidden size.

Dynamic networks DynNNs can adapt their structure based on the input [7]. Early-exiting models control how many layers are used [24] while recursive networks can vary how many times they are executed [8]. Slimming [9], [12] or channel pruning [10], [11] affect the model width, i.e., the number of active nodes in a given layer. Finally, dynamic routing and the mixture of experts (MoE) can switch between different weights [25] or entire subnetworks [26].

DynNNs for audio Several DynNN techniques have been applied to SE and source separation, including early-exiting [13], [27]–[29], recursive networks [14], [30], slimming [16], [31], channel pruning [15] and MoE [18], [32]. A recent work on source separation applied dynamic slimming to the feed-forward layers of transformer blocks [16]. In contrast, we slim a larger part of the network and employ a single router to reduce overhead. We also propose an improved training scheme based on the *Gumbel-softmax trick* [33], [34] and demonstrate its effectiveness with more UFs, resulting in a system that offers greater computational savings and more versatility.

3. DYNAMIC SLIMMABLE DEMUCS

3.1. DEMUCS for Speech Enhancement

Given a single-channel noisy audio signal x of length T , composed of clean speech s and additive noise n , we compute an estimate of the speech \hat{s} using a function \mathcal{M} such that $\mathcal{M}(x) = \hat{s}$. Here, our choice of \mathcal{M} falls on the DEMUCS architecture, initially developed for music source separation [35] and subsequently adapted for real-time monaural speech enhancement [17]. This architecture consists of an encoder, a bottleneck, and a decoder, as shown in Fig. 2.

The encoder is composed of L blocks, each denoted as \mathcal{E}_i , featuring 1D convolution with kernel size K and stride S , ReLU activation,

pointwise 1D convolution, and gated linear unit (GLU) [36]. Each encoder block downsamples the signal by a factor S and doubles its channels, starting from an initial value H . Following a symmetric structure, decoder blocks \mathcal{D}_i feature pointwise 1D convolution, GLU, transposed 1D convolution and — except for the last block — ReLU activation. In order to handle waveform input and output, both \mathcal{E}_1 and \mathcal{D}_1 have a single input and output channel, respectively.

The bottleneck performs sequence modeling on a high-dimensional space comprising $2^{L-1}H$ features. The original DEMUCS employs two long short-term memory (LSTM) units spanning the entire feature space. To reduce the number of trainable parameters and operations, we split the feature space into M equally-sized blocks, assign each block to a separate gated recurrent unit (GRU), and concatenate the resulting output activations into a feature vector with the same dimensionality as the bottleneck input. This is equivalent to employing a single GRU where non-zero values occur only in blocks along the weight matrix diagonals, allowing full connectivity within a block and no connectivity across groups [4], [37]. Lastly, we employ skip connections, as popularized by the U-Net architecture [22], between encoder and decoder blocks, and operate on a version of the input signal x that is upsampled by a factor U and subsequently downsampled.

3.2. Slimmable Encoder-Decoder Blocks

At the core of our blocks, we use slimmable 1D convolution. Each convolutional layer maps a utilization factor, denoted as $v_j \in \mathbb{U}$, to a specific portion of convolutional filters. We define $\mathbb{U} = \{v_j\}_{j=1}^J$ as the discrete set of available UFs of size J . These factors v_j are fractional values ranging from partial utilization, i.e., $v_j < 1$, to full utilization, i.e., $v_j = 1$, controlling the proportion of active weights in the layer. Thus, \mathbb{U} can be treated as an architectural hyperparameter. During inference, the slimmable layers receive a UF as additional input, determining the subset of active filters. Given the convolutional weight tensor $W \in \mathbb{R}^{C_{\text{out}} \times C_{\text{in}} \times K}$, slimming can be applied along the output channels, the input channels, or both. This process involves selecting the first $\lceil C_{\text{out}} v_j \rceil$ output channels and/or $\lceil C_{\text{in}} v_j \rceil$ input channels, depending on the slimming direction.

As shown in Fig. 3a, we slim the first convolution in the encoder block (green) along its output and the pointwise convolution (blue) along its input. Thus, only the block’s internal feature space is slimmed, while its input and output maintain the same dimensionality regardless of UF. In this way, we avoid slimming the GLU, which would cause certain features to be treated as either gating or activation depending on the UF. The decoder block in Fig. 3b follows a similar scheme, preserving the dimensionality of its input and output while slimming internally. However, since the GLU is now applied on the slimmable signal, we employ a slightly different approach for the pointwise convolution (blue). To comply with the GLU structure, we retrieve

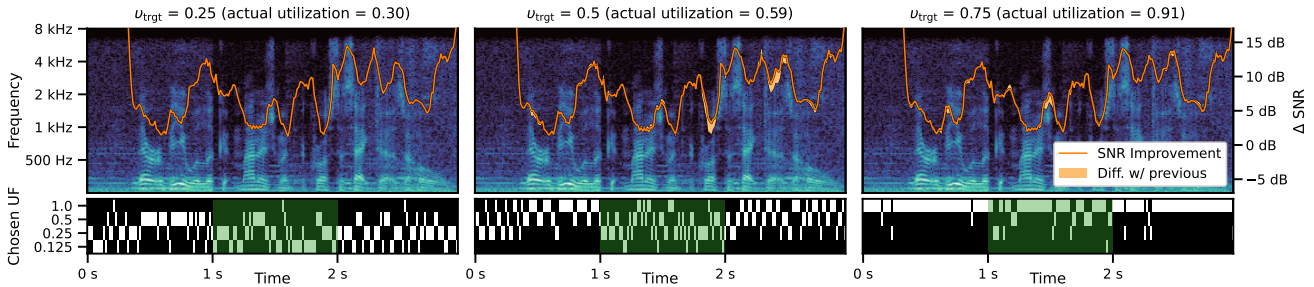


Fig. 4: Example inference for models trained with $v_{\text{trgt}} \in \{0.25, 0.5, 0.75\}$, showing input spectrogram along with improvement in instantaneous SNR (orange line, with yellow regions marking difference with preceding model on the left) and chosen UFs over time. In the middle portion of the sample (in green), we deliberately reduce the noise level by 10 dB to show how each model reacts by decreasing its average utilization.

half of the required weights from the start of the tensor and the other half from the middle, ensuring that the gating portion of the GLU input is always processed with filters associated with it.

3.3. Routing sub-network

The routing module \mathcal{R} , shown in Fig. 2 (red), is tasked with selecting a UF based on the input. It comprises 1D convolution, ReLU activation, diagonal GRU, and point-wise convolution. To limit its computational overhead, we employ diagonal GRUs [38], which can be seen as an extreme case of grouped GRUs where each hidden feature has a separate GRU [37], effectively replacing all matrix multiplications with element-wise products. Furthermore, we match stride and kernel size in the first convolutional layer, decreasing its time resolution and resulting in the downsampled sequence $T^* < T$.

This subnet computes a score matrix $r \in \mathbb{R}^{J \times T^*}$, such that the distribution of UFs for each input frame is given by $\text{softmax}_j(r)$. Since only one UF out of the J available ones is used at any given time, we must turn the aforementioned distribution into discrete decisions. The most straightforward approach involves selecting the UF with the highest probability using the arg max operator. However, this operation is not differentiable, preventing end-to-end training. Furthermore, it results in selections that do not reflect the distribution estimated by \mathcal{R} , causing low-probability UFs to never be chosen. To address both issues, we apply the Gumbel-softmax trick proposed in [33], [34]: during training, we sample from the distribution by adding Gumbel noise to r , ensuring exploration of all available UFs. Differentiation is thus supported through the following relaxation:

$$\mathcal{R}(x) = \begin{cases} \arg \max_j(r + G) & \text{Forward pass} \\ \text{softmax}_j(r + G) & \text{Backward pass} \end{cases} \quad (1)$$

where G is a matrix of i.i.d. Gumbel noise samples. This allows the routing subnet to provide discrete UFs while backpropagating an estimated gradient. During inference, we omit the noise, i.e., $G = 0$.

3.4. Training Strategy

The training process comprises two stages: firstly, we pre-train the slimmable DEMUCS architecture to ensure proficiency in the denoising task for all UFs. Subsequently, we implant the routing subnet \mathcal{R} and train it end-to-end together with the slimmable backbone.

During the first stage, we predict a signal \hat{s}_j using each \mathcal{M}_j , i.e., the model running at utilization v_j . We then compute a denoising loss \mathcal{L}_{SE} for each of the signals \hat{s}_j , and minimize their sum:

$$\mathcal{L}_{\text{Slim}} = \sum_j \mathcal{L}_{\text{SE}}(s, \hat{s}_j) \quad \hat{s}_j = \mathcal{M}_j(x) \quad (2)$$

We employ the loss described in [1], which we found empirically to yield better results than the one originally used by DEMUCS. It

computes the squared distances between predicted and target signals of their complex and magnitude STFTs (with l and f indexing time and frequency bins), both compressed by c and mixed by a factor α :

$$\mathcal{L}_{\text{SE}} = \alpha \sum_{l,f} | |S|^c e^{j\angle_s} - |\hat{S}|^c e^{j\angle_{\hat{s}}} |^2 + (1 - \alpha) \sum_{l,f} | |S|^c - |\hat{S}|^c |^2 \quad (3)$$

In the second stage, we minimize an end-to-end loss comprising the following regularization terms (β and γ are weighting coefficients):

$$\mathcal{L}_{\text{DynSlim}} = \mathcal{L}_{\text{SE}}(s, \hat{s}) + \beta \mathcal{L}_{\text{Eff}} + \gamma \mathcal{L}_{\text{Bal}} \quad (4)$$

The estimated clean speech \hat{s} is computed by combining the output from each UF using $\mathbb{1}_{\mathcal{R}(x)=j}$, an indicator function that is 1 when UF v_j is selected and 0 otherwise, as gating signal. Since $\mathcal{R}(x)$ operates at a lower resolution T^* , we first resample its output to match the bottleneck resolution $\frac{UT}{SL}$ using nearest-neighbor interpolation, followed by zero-order hold to obtain the original input length T :

$$\hat{s} = \sum_j \mathcal{M}_j(x) \cdot \text{upsample}_{T^* \rightarrow T}(\mathbb{1}_{\mathcal{R}(x)=j}) \quad (5)$$

The loss term \mathcal{L}_{Eff} ensures the learned model achieves the defined level of efficiency by keeping the overall utilization close to a target value v_{trgt} . Meanwhile, the balancing term \mathcal{L}_{Bal} , based on [25], prevents the model from favoring only a few UFs. These are:

$$\mathcal{L}_{\text{Eff}} = \left(\sum_j (\tilde{Y}_j v_j) - v_{\text{trgt}} \right)^2, \quad \mathcal{L}_{\text{Bal}} = \frac{1}{J-1} \left(\sum_j \tilde{Y}_j^2 - 1 \right) \quad (6)$$

where $\tilde{Y} \in \mathbb{R}^J$ represents the relative occurrence of each UF across a training batch such that $\tilde{Y}_j = \mathbb{E}(\mathbb{1}_{\mathcal{R}(x)=j})$. We use this because, although we want to favor smaller UFs, we still expect the model to employ bigger UFs on challenging input data, as long as the target efficiency is maintained globally.

4. EXPERIMENTAL SETUP

Data We perform our experiments on the popular VoiceBank+ DEMAND dataset [39]. The training split features 11 572 utterances from 28 speakers, corresponding to ~ 10 hours of data, with background noise mixed at SNRs ranging from 0 dB to 15 dB. We use the utterances from two random speakers as a validation set. The test split contains 824 utterances from 2 unseen speakers mixed with unseen noise at SNRs between 2.5 dB and 17.5 dB. The data is downsampled to 16 kHz. During training, we randomly extract segments of 4 s and augment them based on the DEMUCS training recipe [17].

Model Similarly to the causal variant in the original paper, our DEMUCS backbone is parameterized by $L = 5$, $K = 8$, $S = 4$, and $U = 4$. We decrease the initial hidden channels H to 32 and employ the grouped GRU method described in Section 3.1 with $M = 4$.

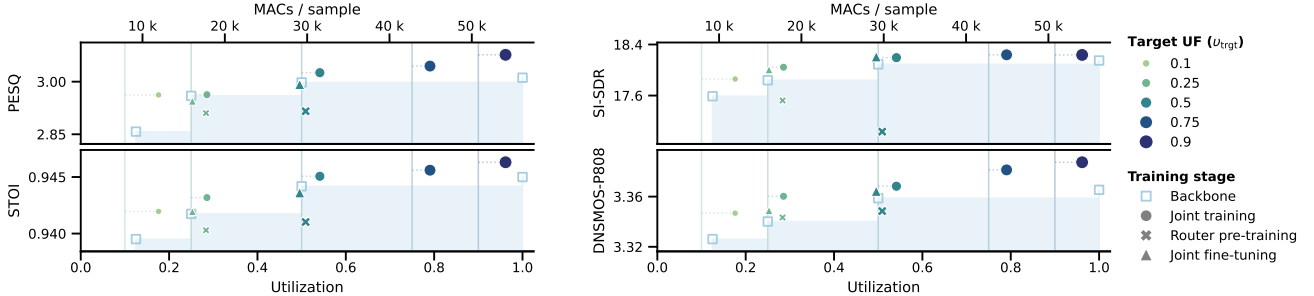


Fig. 5: Pareto fronts given by utilization/MACs (x-axes) vs. speech quality metrics (y-axis) for static slimmable backbone (light blue empty squares) and dynamic models trained on a range of v_{trgt} ; the dotted horizontal lines show the distance between each v_{trgt} (solid vertical lines) and actual average utilization. For $v_{\text{trgt}} \in \{0.25, 0.5\}$, we include results from the alternative training schedule described in Section 4.

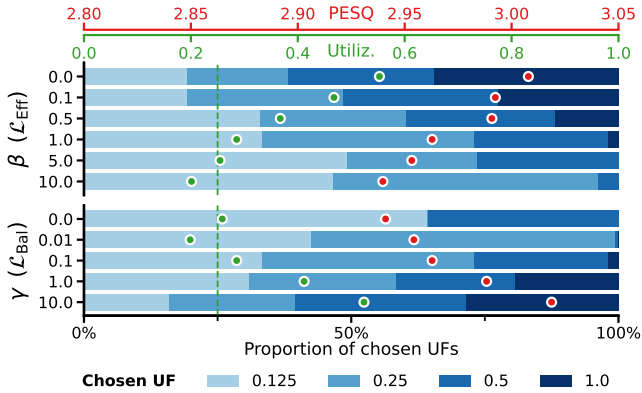


Fig. 6: For models trained with different regularization coefficients (one per row), we show the relative occurrence of each UF (i.e. \tilde{Y}_j ; blue stacked bars) along with their PESQ and avg. utilization (red and green dots, uppermost x-axes); dashed line showing $v_{\text{trgt}} = 0.25$.

For slimming, we set $\mathbb{U} = \{0.125, 0.25, 0.5, 1.0\}$ and thus $J = 4$. The layers in the subnet \mathcal{R} have kernel size of 256 and 64 hidden features/channels, introducing a negligible 0.06 % overhead.

Training During the first stage, we pre-train the slimmable backbone for up to 400 epochs on batches of 32 elements, using a learning rate of 1×10^{-3} that is halved every 15 epochs without improvement on the validation set. In the second stage, we transfer the pre-trained backbone weights, randomly initialize the router, and train both for up to 250 epochs on batches of 16 elements with a learning rate of 1×10^{-3} decaying by a factor of 0.99 per epoch. We also test a variant where the router is pre-trained with the backbone frozen, followed by joint fine-tuning at a learning rate of 1×10^{-4} (✖ and ▲ in Fig. 5). We use $c = 0.3$, $\alpha = 0.3$ for the SE loss (3) (as in the original paper), and set $\beta = 1.0$, $\gamma = 0.1$ for the end-to-end loss (4), based on observations in Fig. 6. In all cases, we use the Adam optimizer and enable early stopping with a patience of 35 epochs.

Metrics We assess speech quality with the perceptual evaluation of speech quality (PESQ) [40], the scale-invariant signal-to-distortion ratio (SI-SDR) [41], the short-time objective intelligibility (STOI) [42], and mean opinion scores predicted using DNSMOS P.808 [43]. For computational efficiency, we estimate multiply-accumulate operations (MACs) per input sample using fvcore².

5. RESULTS

Fig. 5 presents Pareto fronts comparing dynamically-slimmable models trained with different v_{trgt} against the static slimmable backbone. The

dynamic models consistently achieve Pareto efficiency across all metrics, demonstrating improved trade-offs between performance and efficiency. The proposed method is more advantageous when the system is asked to reduce the complexity. For example, when training with $v_{\text{trgt}} = 0.1$ (smallest dot), performance is on par with or better than the backbone with static 0.25 utilization (empty square on line at 0.25) for all metrics. With regularization from \mathcal{L}_{Eff} , the actual utilization is 0.176 on average, resulting in a 29 % reduction in MACs when compared to the static backbone at $UF = 0.25$. Similarly, when training for $v_{\text{trgt}} = 0.9$ (largest dot), the actual utilization averages 0.962, resulting in a 4 % MACs reduction while improving PESQ by 2.2 % and SI-SDR by 0.5 % when compared to the full static backbone (i.e., $UF = 1$). Notably, splitting the second training stage into router pre-training followed by joint fine-tuning achieves better adherence to utilization targets but proves detrimental to speech quality.

The impact of the regularization coefficients used in (4) is shown in Fig. 6. Expectedly, higher β values improve target adherence, which leads to narrower distributions concentrated around small UFs, whereas lower values yield a more diverse selection of UFs, improving PESQ scores despite exceeding v_{trgt} . The choice γ has an analogous yet inverse effect: in both cases, a clear correlation between UF uniformity, average utilization, and speech quality is observed.

Lastly, Fig. 1 demonstrates how a dynamic model adapts its capacity based on input difficulty, indicated there by the initial SI-SDR of noisy inputs. We observe that easier inputs (higher SI-SDR) are processed using lower UFs on average while more capacity is allocated for noisier inputs, leading to larger SI-SDR improvements. Intuitively, this means that resources are spent predominantly on challenging inputs requiring more enhancement while realizing savings on easier ones, reflecting the merit of the proposed architecture. This is further exemplified in Fig. 4, where input regions featuring lower noise levels or less speech content trigger the selection of lower UFs.

6. CONCLUSION

We introduced dynamic slimming to SE, extending the DEMUCS architecture with slimmable blocks and a lightweight routing network. The proposed system dynamically scales to match the complexity of incoming audio, improving quality on challenging inputs while saving resources on easier ones. Our method demonstrates Pareto-optimal behavior across speech quality metrics, offering better trade-offs than static slimming. This highlights the practical value of input adaptiveness and computational scalability, as showcased by our dynamically-slimmable networks, in real-time, resource-constrained settings. We plan to extend this approach to encompass the recurrent bottleneck, leverage the model’s internal representations for routing, and verify its applicability on alternative SE architectures.

²https://github.com/facebookresearch/fvcore/blob/main/docs/flop_count.md

REFERENCES

[1] S. Braun and I. Tashev, "Data Augmentation and Loss Normalization for Deep Noise Suppression," in *Lecture Notes in Computer Science*, 2020.

[2] I. Fedorov, M. Stamenovic, C. Jensen, L.-C. Yang, A. Mandell, Y. Gan, M. Mattina, and P. N. Whatmough, "TinyLSTMs: Efficient Neural Speech Enhancement for Hearing Aids," in *Interspeech 2020*, Oct. 2020.

[3] N. Shankar, G. S. Bhat, and I. M. Panahi, "Real-Time Single-Channel Deep Neural Network-Based Speech Enhancement on Edge Devices," in *Interspeech 2020*, Oct. 2020.

[4] S. Braun, H. Gamper, C. K. Reddy, and I. Tashev, "Towards Efficient Models for Real-Time Deep Noise Suppression," in *ICASSP 2021 - 2021 IEEE International Conference on Acoustics, Speech and Signal Processing (ICASSP)*, Jun. 2021.

[5] R. Yu, Z. Zhao, and Z. Ye, "PFRNet: Dual-Branch Progressive Fusion Rectification Network for Monaural Speech Enhancement," *IEEE Signal Processing Letters*, 2022.

[6] X. Rong, T. Sun, X. Zhang, Y. Hu, C. Zhu, and J. Lu, "GTCRN: A Speech Enhancement Model Requiring Ultralow Computational Resources," in *ICASSP 2024 - 2024 IEEE International Conference on Acoustics, Speech and Signal Processing (ICASSP)*, Apr. 2024.

[7] Y. Han, G. Huang, S. Song, L. Yang, H. Wang, and Y. Wang, "Dynamic Neural Networks: A Survey," *IEEE Transactions on Pattern Analysis and Machine Intelligence*, Nov. 2022.

[8] Q. Guo, Z. Yu, Y. Wu, D. Liang, H. Qin, and J. Yan, "Dynamic Recursive Neural Network," in *2019 IEEE/CVF Conference on Computer Vision and Pattern Recognition (CVPR)*, Jun. 2019.

[9] J. Yu, L. Yang, N. Xu, J. Yang, and T. S. Huang, "Slimmable Neural Networks," in *7th International Conference on Learning Representation*, May 2019.

[10] C. Herrmann, R. S. Bowen, and R. Zabih, "Channel Selection Using Gumbel Softmax," in *Computer Vision – ECCV 2020: 16th European Conference, Glasgow, UK, August 23–28, 2020, Proceedings, Part XXVII*, Aug. 2020.

[11] X. Gao, Y. Zhao, L. Dudziak, R. D. Mullins, and C.-Z. Xu, "Dynamic Channel Pruning: Feature Boosting and Suppression," in *7th International Conference on Learning Representations*, May 2019.

[12] C. Li, G. Wang, B. Wang, X. Liang, Z. Li, and X. Chang, "Dynamic Slimmable Network," in *2021 IEEE/CVF Conference on Computer Vision and Pattern Recognition (CVPR)*, Jun. 2021.

[13] S. Chen, Y. Wu, Z. Chen, T. Yoshioka, S. Liu, J. Li, and X. Yu, "Don't Shoot Butterfly with Rifles: Multi-Channel Continuous Speech Separation with Early Exit Transformer," in *ICASSP 2021 - 2021 IEEE International Conference on Acoustics, Speech and Signal Processing (ICASSP)*, Jun. 2021.

[14] D. Bralias, E. Tzinis, G. Wichern, P. Smaragdis, and J. Le Roux, "Latent Iterative Refinement for Modular Source Separation," in *ICASSP 2023 - 2023 IEEE International Conference on Acoustics, Speech and Signal Processing (ICASSP)*, Jun. 2023.

[15] R. Miccini, C. Laroche, T. Piechowiak, and L. Pezzarossa, "Scalable Speech Enhancement With Dynamic Channel Pruning," in *ICASSP 2025 - 2025 IEEE International Conference on Acoustics, Speech and Signal Processing (ICASSP)*, Apr. 2025.

[16] M. Elmishawi, S. R. Chetupalli, and E. A. P. Habets, "Dynamic Slimmable Network for Speech Separation," *IEEE Signal Processing Letters*, 2024.

[17] A. Défossez, G. Synnaeve, and Y. Adi, "Real Time Speech Enhancement in the Waveform Domain," in *Interspeech 2020*, Oct. 2020.

[18] A. Sivaraman and M. Kim, "Sparse Mixture of Local Experts for Efficient Speech Enhancement," in *Interspeech 2020*, Oct. 2020.

[19] J.-M. Valin, U. Isik, N. Phansalkar, R. Giri, K. Helwani, and A. Krishnaswamy, "A Perceptually-Motivated Approach for Low-Complexity, Real-Time Enhancement of Fullband Speech," in *Interspeech 2020*, Oct. 2020.

[20] D. Stoller, S. Ewert, and S. Dixon, "Wave-U-Net: A Multi-Scale Neural Network for End-to-End Audio Source Separation," in *Proceedings of the 19th International Society for Music Information Retrieval Conference, ISMIR 2018, Paris, France, September 23-27, 2018*, 2018.

[21] M. Sach, J. Franzen, B. Defraene, K. Fluyt, M. Strake, W. Tirry, and T. Fingscheidt, "EffCRN: An Efficient Convolutional Recurrent Network for High-Performance Speech Enhancement," in *Interspeech 2023*, Aug. 2023.

[22] O. Ronneberger, P. Fischer, and T. Brox, "U-Net: Convolutional Networks for Biomedical Image Segmentation," in *Lecture Notes in Computer Science*, 2015.

[23] M. Rusci, M. Fariselli, M. Croome, F. Paci, and E. Flamand, "Accelerating RNN-Based Speech Enhancement on a Multi-core MCU with Mixed FP16-INT8 Post-training Quantization," in *ECML PKDD*, Jan. 2023.

[24] S. Scardapane, M. Scarpiniti, E. Baccarelli, and A. Uncini, "Why Should We Add Early Exits to Neural Networks?" *Cognitive Computation*, Sep. 2020.

[25] W. Fedus, B. Zoph, and N. Shazeer, "Switch Transformers: Scaling to Trillion Parameter Models with Simple and Efficient Sparsity," *J. Mach. Learn. Res.*, Jan. 2022.

[26] N. Shazeer, A. Mirhoseini, K. Maziarz, A. Davis, Q. V. Le, G. E. Hinton, and J. Dean, "Outrageously Large Neural Networks: The Sparsely-Gated Mixture-of-Experts Layer," in *5th International Conference on Learning Representations*, 2017.

[27] A. Li, C. Zheng, L. Zhang, and X. Li, "Learning to Inference with Early Exit in the Progressive Speech Enhancement," in *2021 29th European Signal Processing Conference (EUSIPCO)*, Aug. 2021.

[28] S. Kim and M. Kim, "Bloom-Net: Blockwise Optimization for Masking Networks Toward Scalable and Efficient Speech Enhancement," in *ICASSP 2022 - 2022 IEEE International Conference on Acoustics, Speech and Signal Processing (ICASSP)*, May 2022.

[29] R. Miccini, A. Zniber, C. Laroche, T. Piechowiak, M. Schoeberl, L. Pezzarossa, O. Karrakchou, J. Sparsø, and M. Ghogho, "Dynamic nsNET2: Efficient Deep Noise Suppression with Early Exiting," in *2023 IEEE 33rd International Workshop on Machine Learning for Signal Processing (MLSP)*, Sep. 2023.

[30] M. Kim and T. Kristjansson, "Scalable and Efficient Speech Enhancement Using Modified Cold Diffusion: A Residual Learning Approach," in *ICASSP 2024 - 2024 IEEE International Conference on Acoustics, Speech and Signal Processing (ICASSP)*, Apr. 2024.

[31] M. Elmishawi, S. R. Chetupalli, and E. A. P. Habets, "Slim-Tasnet: A Slimmable Neural Network for Speech Separation," in *2023 IEEE Workshop on Applications of Signal Processing to Audio and Acoustics (WASPAA)*, Oct. 2023.

[32] R. E. Zezario, C.-S. Fuh, H.-M. Wang, and Y. Tsao, "Speech Enhancement with Zero-Shot Model Selection," in *2021 29th European Signal Processing Conference (EUSIPCO)*, Aug. 2021.

[33] C. J. Maddison, A. Mnih, and Y. W. Teh, "The Concrete Distribution: A Continuous Relaxation of Discrete Random Variables," in *5th International Conference on Learning Representations*, Apr. 2017.

[34] E. Jang, S. Gu, and B. Poole, "Categorical Reparameterization with Gumbel-Softmax," in *5th International Conference on Learning Representations*, Apr. 2017.

[35] A. Défossez, N. Usunier, L. Bottou, and F. Bach, "Demucs: Deep Extractor for Music Sources with Extra Unlabeled Data Remixed," Sep. 2019.

[36] Y. N. Dauphin, A. Fan, M. Auli, and D. Grangier, "Language Modeling with Gated Convolutional Networks," in *Proceedings of the 34th International Conference on Machine Learning, ICML 2017, Sydney, NSW, Australia, 6-11 August 2017*, 2017.

[37] M. V. Keirsbilck, A. Keller, and X. Yang, "Rethinking Full Connectivity in Recurrent Neural Networks," May 2019.

[38] Y. C. Subakan and P. Smaragdis, "Diagonal RNNs in Symbolic Music Modeling," in *2017 IEEE Workshop on Applications of Signal Processing to Audio and Acoustics (WASPAA)*, Oct. 2017.

[39] C. Valentini-Botinhao, X. Wang, S. Takaki, and J. Yamagishi, "Investigating RNN-based speech enhancement methods for noise-robust Text-to-Speech," in *9th ISCA Workshop on Speech Synthesis Workshop (SSW 9)*, Sep. 2016.

[40] A. Rix, J. Beerends, M. Hollier, and A. Hekstra, "Perceptual Evaluation of Speech Quality (PESQ) - a New Method for Speech Quality Assessment of Telephone Networks and Codecs," in *2001 IEEE International Conference on Acoustics, Speech, and Signal Processing*, May 2001.

[41] J. Le Roux, S. Wisdom, H. Erdogan, and J. R. Hershey, "SDR – Half-baked or Well Done?" in *ICASSP 2019 - 2019 IEEE International Conference on Acoustics, Speech and Signal Processing (ICASSP)*, May 2019.

[42] C. H. Taal, R. C. Hendriks, R. Heusdens, and J. Jensen, "A Short-Time Objective Intelligibility Measure for Time-Frequency Weighted Noisy Speech," in *2010 IEEE International Conference on Acoustics, Speech and Signal Processing*, 2010.

[43] C. K. A. Reddy, V. Gopal, and R. Cutler, "DNSMOS: A Non-Intrusive Perceptual Objective Speech Quality Metric to Evaluate Noise Suppressors," in *ICASSP 2021 - 2021 IEEE International Conference on Acoustics, Speech and Signal Processing (ICASSP)*, Jun. 2021.